



## University of Tennessee, Knoxville Trace: Tennessee Research and Creative Exchange

---

Masters Theses

Graduate School

---

12-2015

# Preparation and Characterization of Thermodynamically Controlled Polymer Nanocomposites

Jiadi Hou

*University of Tennessee - Knoxville*, [jhou7@vols.utk.edu](mailto:jhou7@vols.utk.edu)

---

### Recommended Citation

Hou, Jiadi, "Preparation and Characterization of Thermodynamically Controlled Polymer Nanocomposites." Master's Thesis, University of Tennessee, 2015.  
[https://trace.tennessee.edu/utk\\_gradthes/3586](https://trace.tennessee.edu/utk_gradthes/3586)

This Thesis is brought to you for free and open access by the Graduate School at Trace: Tennessee Research and Creative Exchange. It has been accepted for inclusion in Masters Theses by an authorized administrator of Trace: Tennessee Research and Creative Exchange. For more information, please contact [trace@utk.edu](mailto:trace@utk.edu).

To the Graduate Council:

I am submitting herewith a thesis written by Jiadi Hou entitled "Preparation and Characterization of Thermodynamically Controlled Polymer Nanocomposites." I have examined the final electronic copy of this thesis for form and content and recommend that it be accepted in partial fulfillment of the requirements for the degree of Master of Science, with a major in Chemistry.

Mike Kilbey, Major Professor

We have read this thesis and recommend its acceptance:

Jimmy Mays, Ampofo Darko

Accepted for the Council:

Carolyn R. Hodges

Vice Provost and Dean of the Graduate School

(Original signatures are on file with official student records.)

---

**Preparation and Characterization of  
Thermodynamically Controlled Polymer Nanocomposites**

**A Thesis Presented for the  
Master of Science  
Degree  
The University of Tennessee, Knoxville**

**Jiadi Hou  
December 2015**

## **ABSTRACT**

The mechanical and physical properties of polymeric materials can be greatly improved by adding nanoscale additives. To mediate the dispersion of nanoparticles in polymers, it is often necessary to modify their surfaces to prevent aggregation. While polymer nanocomposites system consisting of homopolymer-grafted nanoparticles are well understood, copolymer-functionalized nanoparticles are less well understood but provide additional ways to alter dispersion through the use of chemically different comonomers. In this thesis, polystyrene nanocomposites blended with copolymer-grafted nanoparticles were prepared and studied. The particular comonomers used were methyl methacrylate and cyclohexyl methacrylate, which provides miscibility with polystyrene. Polymers with varying comonomer ratios were synthesized via atom transfer radical polymerization and grafted onto silica nanoparticle surfaces. The functionalized particles were then dispersed into polystyrene to make polymer nanocomposites. The resulting materials were characterized by differential scanning calorimeter and atomic force microscopy and the role of the grafted polymer composition on the glass transition temperature of the nanocomposites and the dispersion state of the nanoparticles was examined. These results provide preliminary insight into how random copolymers can affect polymer nanocomposite structure and properties.

# TABLE OF CONTENTS

CHAPTER I INTRODUCTION AND BACKGROUND .....	1
1.1 Polymer nanocomposites with polymer-grafted nanoparticles.....	4
1.1.1 Bare spherical nanoparticles .....	4
1.1.2 Homopolymer-grafted nanoparticles .....	6
1.1.3 Copolymer-grafted nanoparticles.....	8
1.2 Goals of work.....	12
CHAPTER II EXPERIMENTAL METHODS.....	15
2.1 Preparation of polymer nanocomposites.....	16
2.1.1 Synthesis of P(MMA- <i>ran</i> -CHMA) via ATRP .....	17
2.1.2 Synthesis of Silica Nanoparticles.....	18
2.1.3 Functionalization of Silica Nanoparticles with epoxy group.....	19
2.1.4 Preparation of copolymer-grafted nanoparticles.....	20
2.1.5 Fabrication of polymer nanocomposites .....	21
2.2 Characterization .....	21
CHAPTER III RESULTS AND DISCUSSION.....	23
3.1 Characterization of P(MMA- <i>ran</i> -CHMA).....	24
3.1.1 Molecular weight and PDI.....	24
3.1.2 Comonomer ratio of the random copolymers .....	25
3.2 Characterization of copolymer-grafted nanoparticles.....	28
3.2.1 Size of bare silica nanoparticles.....	28

3.2.2 Grafting density of copolymer-grafted nanoparticles .....	29
3.3 Characterization of polymer nanocomposites.....	33
3.3.1 Glass transition temperature .....	33
3.3.2 Dispersion state of nanoparticles in polymer matrices .....	34
CHAPTER IV CONCLUSIONS AND FUTURE WORK.....	40
4.1 Conclusion .....	41
4.2 Future work.....	42
REFERENCE.....	44
VITA.....	47

## LIST OF TABLES

Table 2.1. Reaction conditions to achieve P(MMA- <i>ran</i> -CHMA) with various molecular weights. ....	18
Table 2.2. Formulations of comonomers used to develop random copolymers of different monomer ratio. ....	18
Table 2.3. Molecular weight cut-off (MWCO) of dialysis tubing membrane for P(MMA- <i>ran</i> -CHMA) of various molecular weight. ....	20
Table 3.1. Molecular weight of P(MMA- <i>ran</i> -CHMA) determined by GPC. ....	24
Table 3.2. Composition of comonomers determined by <sup>1</sup> H NMR. ....	28
Table 3.3. Calculated radius of the silica nanoparticles. ....	29
Table 3.4. Mass and volume data to determine the density of silica nanoparticles. ....	31
Table 3.5. Glass transition temperature of nanocomposites samples. ....	34

## LIST OF FIGURES

Figure 1.1. Schematic illustration of a wet brush condition (left) and a dry brush condition (right). .....	7
Figure 1.2. Representative phase diagrams of homopolymer-grafted spherical nanoparticles dispersed in a chemically identical polymer matrix: (a) $\varepsilon = 0.5$ , $\nu N^2/R_g^3 = 1.0$ ; (b) $\varepsilon = 5.0$ , $\nu N^2/R_g^3 = 1.0$ ; (c) $\varepsilon = 0.5$ , $\nu N^2/R_g^3 = 0.1$ . Taken from reference 11. ....	9
Figure 1.3. Schematic showing how variation on blockiness was examined in A-B copolymer grafts. The blockiness decreases from top to bottom. (Image taken from reference 15.) .....	11
Figure 2.1. Schematic illustration of the fabrication of PS based nanocomposites.....	16
Figure 2.2. Schematic demonstration of ATRP process initiated by HEBiB. The resulting polymer is functionalized with hydroxyl group which is used to graft chains onto the surface of silica nanoparticles. ....	18
Figure 3.1. GPC traces of P(MMA- <i>ran</i> -CHMA) with composition ratio 80:20 CHMA:MMA polymerized under different conditions.....	25
Figure 3.2. $^1\text{H}$ NMR spectra of P(MMA- <i>ran</i> -CHMA) with feed ratio of 80:20 at the start (top) and the end (bottom) of the polymerization. ....	27
Figure 3.3. Results of dynamic light scattering measurements of the silica nanoparticles in DI water. ....	29



Figure 3.4. TGA curve showing the mass loss of copolymer-grafted nanoparticles modified with 10k polymer brushes (CHMA:MMA 80:20).....	30
Figure 3.5. A linear regression graph of volume versus mass. Density can be determined by the slope of the trend line.....	31
Figure 3.6. TGA curve showing the mass loss of epoxy-coated nanoparticles. ....	33
Figure 3.7. DSC curves of 18k PS and 18k PS blended with nanoparticles grafted with 10k brushes of various composition. Sample numbers correspond to those in Table 3.5. Data was analyzed using <i>TA Universal Analysis</i> software. ....	35
Figure 3.8. AFM images of PS nanocomposites made with 10k copolymer-grafted nanoparticles in a matrix of 18k. The loading ratio is 2 wt. %. From 1 to 5, the ratios of MMA units in the brush are: 0%, 5%, 10%, 15%, and 20%. ....	39

**CHAPTER I**  
**INTRODUCTION AND BACKGROUND**

It is widely admitted that the mechanical and physical properties of polymeric materials can be greatly enhanced by adding nanoscale organic or inorganic additives, such as carbon black, silicate nanolayers, and silica nanoparticles. As a combination of polymer science and nanotechnology, polymer matrix based nanocomposites exhibit a large range of potential applications, including light-weight materials, flame resistant materials, and fuel cell electrodes. Polymer nanocomposites attract much attention in the field of material science because they create new ways to design innovative materials and offer many opportunities to optimize the properties of the polymeric materials. In addition to the choice of the matrix material, many factors affect the properties of the polymer nanocomposite, such as the shape and dimension of the nanoparticles, the spatial correlations between the nanoparticle locations, and the molecular weight and polydispersity of the polymer matrix.

How various interactions at the nanoscale affect the structure and properties of polymer nanocomposites remains a challenge. Understanding how to design materials that possess appropriate interactions is necessary to effectively optimize the resultant polymeric nanocomposite system. A variety of experimental discoveries on simple systems have led the way, and theory, simulation and modeling have been used to describe the structure of multi-component polymer-decorated nanoparticle systems, including molecular simulations<sup>1</sup>, density functional theory (DFT)<sup>2</sup>, self-consistent field theory (SCFT)<sup>3</sup>, and polymer reference interaction site model (PRISM)<sup>2</sup>. The use of simulation, modeling and theory provides an effective way to explore behaviors, allowing important insights into

design features that regulate structure and properties of polymer nanocomposites. These sets of studies have allowed factors such as the role of nanoparticle curvature on miscibility of the nanoparticles within the polymer matrix, the role of polydispersity and copolymer design and the effect of interfaces on the phase behavior of polymer nanocomposites to be examined rather easily because the availability of computing power provides an efficient way to explore the wide parameter space that governs complex systems.

Although the incorporation of nanoparticles introduces an innovative way of designing new functional materials, achieving desirable properties remains a significant challenge. Controlling the morphological structure of polymer nanocomposites requires the ability to tailor the spatial distribution of the nanoparticles within the polymer host. One strategy to achieve this goal is to graft chains onto the surfaces of the nanoparticles.<sup>2</sup> The functionalization of the nanoparticles offers an opportunity to tune the interaction between the free chains and grafted chains by controlling the number of grafted chains per area, the degree of polymerization of the grafted chains,  $N$ , and of the polymer matrix,  $P$ , as well as the nanoparticle size, shape and dimension. The role of each factors on the structure and properties of the polymer nanocomposites will be discussed in detail in the following sections. These variables make up an enormous design space, which is why careful research into the role of polymer design and grafting is needed.

## **1.1 Polymer nanocomposites with polymer-grafted nanoparticles**

Due to its simplicity, it would be appropriate to start the discussion with a special case involving bare spherical particles incorporated with polymer matrix. The earliest application can be found even before the word ‘nanotechnology’ was widely used. Payne studied the dynamic properties of rubbers blended with carbon black.<sup>4</sup> By varying the mixing time, the dynamic modulus and dynamic viscosity, as well as other dynamic properties of rubber, were reduced. These and other studies of polymer nanocomposites containing bare, unfunctionalized particles showing that the addition of nanomaterials altered materials properties established the foundation for subsequent efforts based on polymer-functionalized nanoparticles in polymer hosts.

### ***1.1.1 Bare spherical nanoparticles***

The organization of bare particles within the polymer hosts depends on the radius of the nanoparticle,  $R$ , and volume fraction,  $\phi$ , in a homopolymer matrix with the degree of polymerization,  $P$ .<sup>5</sup> In the ideal sense, entropy favors particle dispersion due to the increases randomness when the particles are mixed with polymer chains; however in realistic cases, interactions can make the nanoparticles immiscible with the polymer hosts.

For example, depletion interactions can drive aggregation of nanoparticles when polymers are not adsorbed onto the particles surfaces. Depletion interactions arise when the distance between two nanoparticles is smaller than the characteristic size of the

polymer chains. In this case, rather than adopt a configuration that is distorted from their equilibrium configuration, the chains exit the gap between the particles, causing aggregation, hence phase separation.<sup>2</sup> Bridging interactions can also drive aggregation. Bridging interactions occur in situations where polymer chains adsorb on particle surfaces. As a result, polymers form strongly bound layers, which decreases the miscibility of the nanoparticles in the polymer matrix. The number of bridges decreases with the particle size. Hence, bridging interactions become insignificant as the size of the particles decreases.<sup>2</sup>

In most practical situations involving polymer nanocomposites, the nanoparticles exhibit a very strong tendency to aggregate due to van der Waals interactions between the bare nanoparticles. This attractive interaction greatly contributes to the tendency of inorganic nanoparticles to aggregate. The van der Waals interaction potential may be expressed as:

$$V(x_d) = -A_H R / 6x_d \quad (1)$$

where  $A_H$  is the Hamaker constant and  $x_d$  is the distance of separation between the centers of the cores.<sup>6</sup> Equation 1 shows that as the distance between nanoparticles decreases, the strength of the attraction dramatically increases. Because of the dominance of van der Waals surface forces, it is necessary to devise ways to modify nanoparticle surfaces to prevent aggregation. One way to screen these interactions is to functionalize the nanoparticles with layers of tethered polymer chains, which are often called “polymer brushes”.

### 1.1.2 Homopolymer-grafted nanoparticles

As suggested above, grafting polymer brushes onto nanoparticles has been found to be a very effective way to screen van der Waals interactions between nanoparticles, thereby stabilizing the dispersion. The miscibility of homopolymer-grafted nanoparticles within a polymer matrix is determined by factors such as nanoparticle shape and size, grafting density of chains, the degrees of polymerization of the grafted chains,  $N$ , and of the polymer matrix,  $P$ .<sup>7, 8</sup> Although the characteristics of the nanoparticle matter, the easiest case to understand is the situation where polymers are tethered onto flat surfaces. (In other words, for simplicity, the nanoparticle curvature is not considered.)

For low grafting densities, polymer chains with  $N$ -mer grafted onto the surface form a “mushroom” structure of a radius  $R_{\text{mush}}$ . The free energy of such a system can be expressed as:

$$F/k_{\text{B}}T \approx R_{\text{mush}}^2/Na^2 + (N/P)(Na^3/R_{\text{mush}}^3) \quad (2)$$

where  $a$  is the characteristic monomer size,  $R_{\text{mush}}^2/Na^2$  describes the penalty for elastic stretching (deformation of the chain), and  $(N/P)(Na^3/R_{\text{mush}}^3)$  captures the entropic excluded volume contribution.<sup>9</sup> As observed from Equation 2, the ratio between the length of brushes and the host chains,  $N/P$ , plays an important role. When  $N/P > 1$ , the free chains (having degree of polymerization  $P$ ) are shorter than the grafted chains. In this case, the free (matrix) chains are able to penetrate into the brush layer due to a favorable entropic potential (mixing). Hence, the grafted chains stretch to accommodate incoming short matrix chains. This situation is called a “wet brush”. When  $N/P < 1$ , the

grafted chains are shorter than the free chains and as a result, the grafted chains are compressed. The grafted chains form a condensed brush layer, which expels free chains from the brush layer. In this case, the “dry brush” condition is met.

Dry brush conditions also occur as the grafting density becomes high. In this case, functionalization leads to surfaces that are crowded with tethered chains ( $N$ -mer chains) which makes it impossible for the free chains ( $P$ -mers) to penetrate into the grafted layer. However, if the curvature of the surface is taken into consideration, the situation would be different. Simulations by Nodoro *et al.* suggest that for a constant grafting density, the free chains exhibit higher penetrability into the grafted layer with increasing nanoparticle curvature, because the crowding of chains is reduced compared to a flat surface.<sup>10</sup>

Based on these arguments, it stands to reason that the miscibility of nanoparticles within the polymer matrix should be high when wet brush conditions are met and low when dry brush conditions dominate. These two situations are drawn in Figure 1.1.

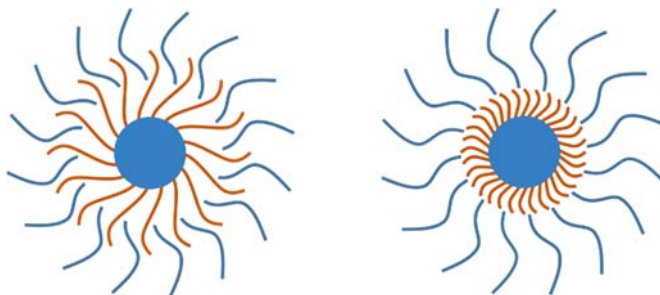


**Figure 1.1. Schematic illustration of a wet brush condition (left) and a dry brush condition (right).**



Polymer grafted nanoparticles can display unusual self-assembly behaviors when the nanoparticle surface contains bare patches. In this situation, having exposed areas on the nanoparticles brings into play surface/polymer interactions that are different from the grafted-polymer/matrix polymer interactions. The relative difference in the strength and range of these two interactions can dominate the spatial distribution of the nanoparticles. To understand the above behaviors, a morphological phase diagram can be depicted with four nondimensional parameters (Figure 1.2):  $\varepsilon$ , interaction energy between two particles, in unit of  $k_B T$ ;  $R/R_g$ , where  $R_g$  is the radius of gyration of nanoparticles;  $n_p$ , the number of grafted chains per particle; and  $\nu N^2/R_g^3$ , a nondimensional excluded volume parameter.<sup>11</sup> With the various combinations of these four parameters, nanoparticles may exhibit freely dispersed particles (*D*); stringlike morphologies (*C*); hexagonally packed sheetlike morphologies (*H*); square-lattice packed sheetlike morphologies (*S*); and densely packed aggregates (*A*).

### ***1.1.3 Copolymer-grafted nanoparticles***

The above studies were established based on the behavior of nanoparticles functionalized with relatively monodisperse homopolymer grafts in a matrix polymer of the same chemical type. Another important situation is when the chemical design of the grafted copolymer differs from that of the host polymer (matrix polymer). These types of studies of the effect of copolymer functionalized nanoparticles in a polymer matrix have recently captured the interest of researchers. Compared to homopolymer functionalization,

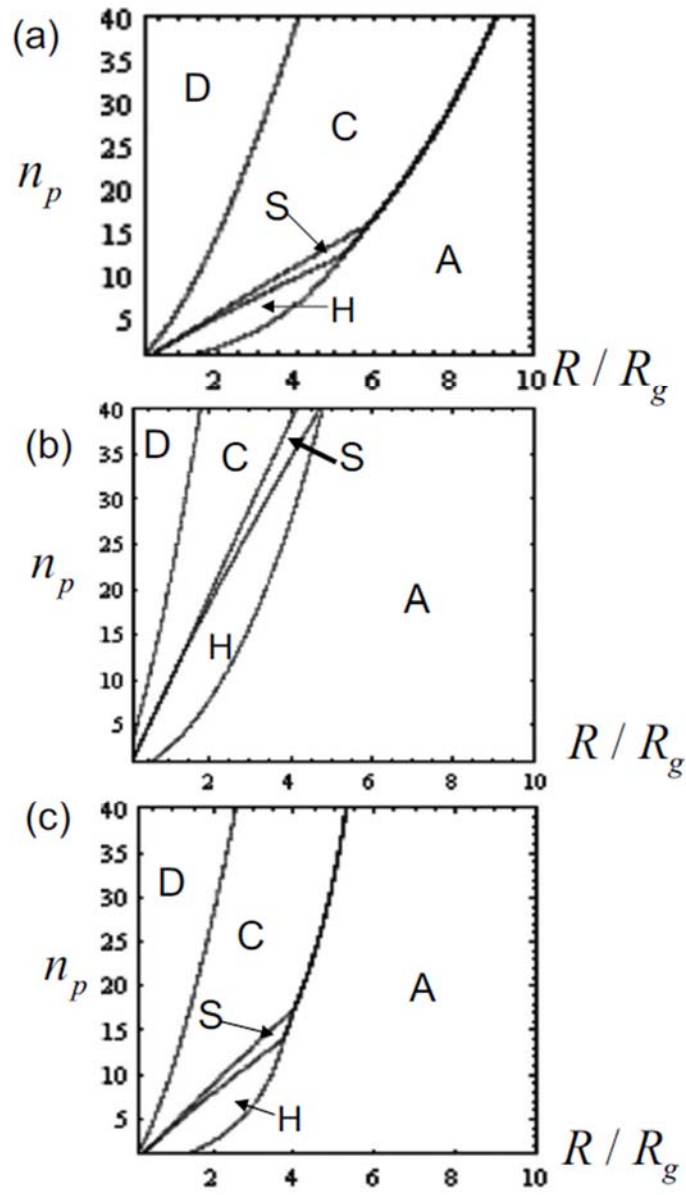


**Figure 2.2. Representative phase diagrams of homopolymer-grafted spherical nanoparticles dispersed in a chemically identical polymer matrix: (a)  $\varepsilon = 0.5, \nu N^2/R_g^3 = 1.0$ ; (b)  $\varepsilon = 5.0, \nu N^2/R_g^3 = 1.0$ ; (c)  $\varepsilon = 0.5, \nu N^2/R_g^3 = 0.1$ . Taken from reference 11.**

copolymer functionalization is more complicated because it introduces more than one type of monomer unit onto the surface of nanoparticles, thereby creating additional tunability through control of brush composition and copolymer design. Given the vast number of monomers of different types that can be incorporated into polymers (and, therefore, into surface grafted polymers) using modern polymerization methods,<sup>12</sup> varying the graft sequence or overall composition of the comonomer provides more possibilities and variations in fabricating functional materials.

Although there are a few examples in which copolymer-grafted nanoparticles have been successfully prepared,<sup>13, 14</sup> most of the research on the properties of copolymer-grafted nanoparticles in polymer matrices has been done by simulation. Jayaraman studied the influence of copolymer-functionalized nanoparticles on the polymer matrix via PRISM and Monte Carlo (MC) simulations.<sup>15</sup> All simulations were conducted under the conditions that a) spherical nanoparticles were grafted with AB copolymers (with A monomer attached to particle surface) and b) A-A and B-B attractive interactions were present. The copolymer-grafted nanoparticles were dispersed in either A or B homopolymer matrix. In the presence of insignificant A-B repulsion, the alternating A-B copolymer-grafted nanoparticle forms an isotropic nanocluster. In the case where the graft copolymer consists of an A-B diblock, the A block forms compact clusters near the nanoparticle surface while the outer B block chains form loose clusters. If the A-B repulsion becomes strong, the cluster of diblock sequences does not change, while the alternating brushes results in either dispersion of particles or formation of clusters.

Jayaraman and coworkers also studied the effect of copolymer sequence by varying blockiness, which is defined as the length of each block, at constant grafting length, as seen in Figure 1.3. The structure of grafted chains was studied with copolymer-nanoparticles dispersed in A or B homopolymer matrix. In the situation where A-A or B-B monomer-monomer contacts are attractive but A-B repulsion is negligible, the cluster size decreases as the blockiness increases. On the other hand, in situations in which both A-A and B-B attractions are present, the cluster size remains constant. When A-B repulsion becomes significant, the cluster size increases with an increasing blockiness.<sup>16</sup>

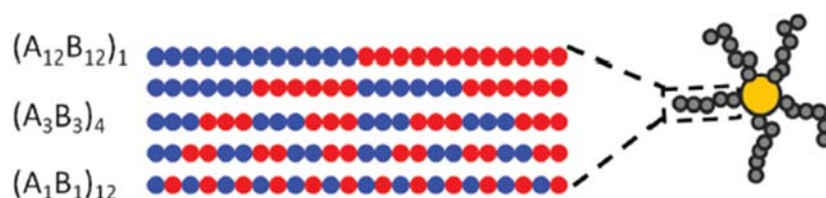


**Figure 3.3. Schematic showing how variation on blockiness was examined in A-B copolymer grafts. The blockiness decreases from top to bottom. (Image taken from reference 15.)**

These studies show that chemical heterogeneity in grafted chains plays an important role in tuning the interactions between particles and the properties of the resultant polymer nanocomposites. Because the incorporation of copolymers offers more possibilities in terms of fabricating materials based on controlling interactions, much work is needed to quantitatively understand the effect of monomer sequence, grafting density, or the polydispersity of polymer matrix on the polymer nanocomposites.

## 1.2 Goals of work

My work is to understand how copolymer-functionalized nanoparticles affect the glass transition temperature ( $T_g$ ) of the nanocomposites and the role of annealing on the dispersion of the nanoparticles. Polystyrene (PS) will be used as the polymer matrix, and a random copolymer of methyl methacrylate and cyclohexyl-methacrylate, P(MMA-*ran*-CHMA), will be tethered onto the surface of a silica. P(MMA-*ran*-CHMA) is an interesting material because PS is immiscible with PMMA, but miscible with PCHMA.<sup>17</sup> Making a random copolymer of MMA and CHMA provides an easy way to tune the interaction of the random copolymer with PS from immiscible to miscible. The ability to span this thermodynamic phase space is novel. To accomplish my studies I will be investigating how P(MMA-*ran*-CHMA) of various comonomer ratio affects the  $T_g$  of the PS nanocomposites and the dispersion state of the nanoparticles.

My work focuses on linear polymers and copolymers, and to synthesize the necessary polymers, the controlled/living radical polymerization method known as atom transfer radical polymerization (ATRP) will be used. ATRP is an ideal choice for my research because it allows polymers of desired molecular weight, and low polydispersity index (PDI) to be prepared under mild reaction conditions.<sup>18</sup> More importantly, methacrylates are useful monomers in terms of their high polymerizability by ATRP.<sup>18</sup>

After the polymers are prepared, they will be grafted onto silica nanoparticle surfaces via “grafting to” method. The grafting to method has the advantage of a facile and modular

approach. It allows polymers to be thoroughly characterized prior to grafting, and grafting density can be easily manipulated by varying the reaction time. To gain an understanding of how the composition of polymer brushes affect the dispersion state of copolymer-grafted nanoparticles, polymer chains of various molecular weights and comonomer ratios will be used. The copolymer decorated silica nanoparticles will be dispersed into polymer matrices and basic properties of the polymer nanocomposite examined.

Several types of measurements will be used to complete my research. Gel permeation chromatography (GPC) measurements will be used to determine the number average molecular weight ( $M_n$ ), the weight average molecular weight ( $M_w$ ), and polydispersity index, PDI, of the P(MMA-*ran*-CHMA) polymers. Nuclear magnetic resonance (NMR) spectroscopy will complement the GPC measurements by providing the ratio of the comonomers in the random copolymer. Dynamic light scattering (DLS) will be used to measure the size of silica nanoparticles. Thermo-gravimetric analysis (TGA) will be used to assess grafting density of chains from the mass loss and differential scanning calorimeter (DSC) will be used to determine the glass transition temperature ( $T_g$ ) of the polymer nanocomposites. Atomic force microscopy (AFM) will be used to gain insight into arrangement of copolymer grafted nanoparticles in the polymer nanocomposites.

If my research succeeds in understanding the influence of copolymer-grafted nanoparticles on the  $T_g$  of the polymer matrix and dispersion state of the nanoparticles, it

may unlock the potential to develop innovative polymeric composite materials for applications in mechanical, optical, and biological contexts, ranging from surgical sutures, implant scaffolds, structural members, advanced membranes, or sensors, to name just a few examples.

## **CHAPTER II**

### **EXPERIMENTAL METHODS**



In this chapter, the fabrication method used to make my polymer nanocomposites will be introduced. First, and as shown in Figure 2.1, silica nanoparticles are prepared and then decorated with epoxy group by reacting with (3-glycidyloxypropyl)trimethoxysilane (GLYMO) in a solution of tetrahydrofuran (THF). Next, random copolymers functionalized with hydroxyl end group that were synthesized via ATRP were reactively coupled onto the nanoparticle surface. The resulting copolymer-grafted nanoparticle is recovered by dialysis. To make nanocomposites, the copolymer-grafted nanoparticles are dispersed in a solution that also contains PS homopolymer. Finally, after the solvent is removed by evaporation, the polymer nanocomposites is fabricated. These basic steps are covered in more detail in the remaining sections of this chapter.

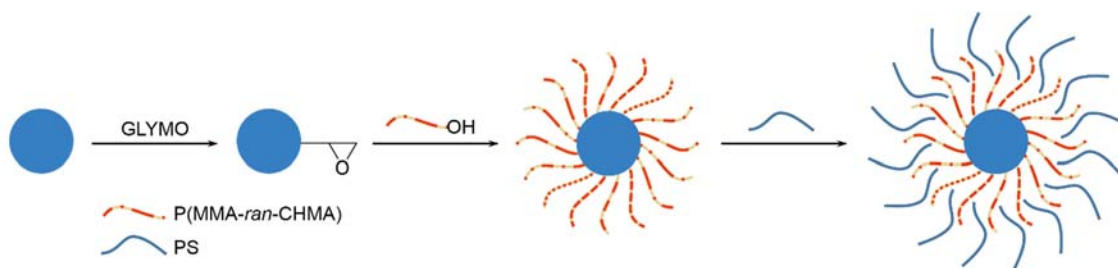


**Figure 2.1. Schematic illustration of the fabrication of PS based nanocomposites.**

## 2.1 Preparation of polymer nanocomposites

All reagents, except methyl methacrylate (MMA) and cyclohexyl-methacrylate (CHMA), were purchased from Aldrich and used without further purification or preparation. MMA and CHMA were purified by passing these monomers through basic aluminum columns to remove any inhibitor. Dialysis tubing made of regenerated cellulose was purchased

from Spectrum Laboratories, Inc. and stored in 1% sodium benzoate solution according to the manufacturer's instruction.

### ***2.1.1 Synthesis of P(MMA-ran-CHMA) via ATRP***

5.0 mg ( $3.5 \times 10^{-2}$  mmol) CuBr, the appropriate monomer (or comonomers), 15  $\mu$ L *N,N,N',N'',N''*-pentamethyldiethylenetriamine (PMDETA), 5  $\mu$ L ( $3.45 \times 10^{-2}$  mmol) 2-hydroxyethyl 2-bromoisobutyrate (HEBiB) and 3.5 mL anisole were added to a 3-neck round bottom flask then followed by three freeze-pump-thaw processes to remove dissolved oxygen. The flask was sealed with a rubber septum and placed in an oil bath thermostated at 50 °C for 80 minutes to achieve molecular weight of 10 kg/mol. If the reaction was performed at 55 °C for 60 minutes, polymers having molecular weight of 22 kg/mol were obtained. HEBiB is a functional initiator that contains a hydroxyl group at the terminus. The hydroxyl group does not participate in polymerization, and as a result, using HEBiB creates polymers with a single hydroxyl end group, which is used to graft the polymer chains to the surface of nanoparticles. The polymerization process is shown in Figure 2.2. By varying the ratio of comonomers, random copolymer of different composition can be prepared, and the particular compositions that I used are shown in Table 2.1 and 2.2.

After the ATRP reaction was stopped by removing the rubber septum to allow oxygen in, the solution was passed through an aluminum column to remove CuBr and then the solvent was removed by evaporation. The recovered polymers were redissolved in

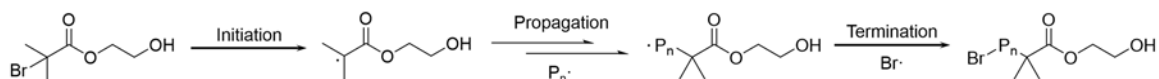


**Figure 2.2. Schematic demonstration of ATRP process initiated by HEBiB. The resulting polymer is functionalized with hydroxyl group which is used to graft chains onto the surface of silica nanoparticles.**

**Table 2.1. Reaction conditions to achieve P(MMA-*ran*-CHMA) with various molecular weights.**

Target $M_n$ kg/mol	Monomer mmol	Initiator mmol	M/I	Reaction time min	Temperature °C	Conversion %
10	17.37	$3.45 \times 10^{-2}$	503	80	50	13
22	10.94	$3.45 \times 10^{-2}$	317	60	55	50
34	17.37	$3.45 \times 10^{-2}$	503	60	55	45

**Table 2.2. Formulations of comonomers used to develop random copolymers of different monomer ratio.**

Feed ratio $f_{CHMA} : f_{MMA}$	CHMA mmol	MMA mmol	CHMA/MMA
80:20 = 4	13.90	3.47	4.00
85:15 = 5.6	14.76	2.60	5.68
90:10 = 9	15.62	1.74	8.98
95: 5 = 19	16.49	0.86	19.17

dichloromethane and precipitated into hexane three times. Finally, the non-solvent hexane was removed by decanting and the recovered, purified polymers were dried under vacuum.

### 2.1.2 Synthesis of Silica Nanoparticles

The procedure I used is based on the method developed by Hartlen and coworkers.<sup>19</sup> 9.1 mg L-arginine was dissolved into 6.9 mL H<sub>2</sub>O. Then 0.45 mL of cyclohexane was added

and the solution was heated to 60 °C. 0.55 mL of tetraethyl orthosilicate (TEOS) were added and the temperature was maintained while the solution was stirred for 20 hours. After cooling, the product was precipitated into hexane, recovered and then redissolved in THF followed by separation by centrifugation to get rid of the liquid. This process was repeated 3 times. The recovered silica nanoparticles were dried at 100 °C under vacuum for 12 hours then dissolved in 6 mL of H<sub>2</sub>O. The concentration of the resulting solution is 0.693 g/mL.

### ***2.1.3 Functionalization of Silica Nanoparticles with epoxy group***

The following procedure represents a modification of the method developed by Lin and coworkers.<sup>20</sup> To prepare the silica nanoparticles for the “grafting to” process, the nanoparticles are decorated with epoxy groups. To accomplish this, 75 µL trimethylamine (TEA), 0.7 mL of the silica nanoparticles, and 0.5 mL of GLYMO were added into 24 mL tetrahydrofuran (THF). The solution was refluxed for 10 hours in a flask equipped with a condenser unit. After cooling, the product was precipitated into hexane, recovered and then redissolved in THF, followed by separation by centrifugation, which allows excess liquid to be removed. This process was repeated 3 times to purify the epoxy-decorated nanoparticles. The recovered nanoparticles were dried at 100 °C under vacuum for 12 hours.

#### **2.1.4 Preparation of copolymer-grafted nanoparticles**

To attach end-functionalized polymer chains to epoxy-decorated nanoparticles, 0.5 g of P(MMA-*ran*-CHMA) made to have a hydroxyl end group and 0.5 g of epoxy-coated silica nanoparticles were added into 50 mL of dimethylformamide (DMF) and refluxed for 12 hours. After the reaction was stopped by removing the heat, the solution was purified by dialysis for 7 days to remove free (non-bonded) polymer chains. In order to enable free (non-bonded) polymer chains to be removed, the dialysis tubing was chosen to have a molecular weight cut-off (MWCO) slightly greater than the molecular weight of the free chain, but smaller than twice the molecular weight of the free chain (as shown in Table 2.2), which was used to represent the molecular weight of a polymer-grafted nanoparticle having two or more chains attached. The solution was precipitated into hexane and redissolved in THF three times, after which the copolymer-functionalized nanoparticles were recovered by centrifugation. The solid residue was dried at 100 °C under vacuum.

**Table 2.3. Molecular weight cut-off (MWCO) of dialysis tubing membrane for P(MMA-*ran*-CHMA) of various molecular weight.**

$M_n$ of P(MMA- <i>ran</i> -CHMA)	MWCO of Dialysis tubing
10 kg/mol	15 kg/mol
22 kg/mol	25 kg/mol
34 kg/mol	50 kg/mol

### ***2.1.5 Fabrication of polymer nanocomposites***

Polymer nanocomposites having a nanoparticle loading ratio of 2 wt. % were made by adding 0.2 g of PS (matrix) and 4 mg of copolymer-grafted nanoparticles into 0.5 mL of THF. The mixture was ultrasonicated for 2 hours to disperse the polymer-grafted nanoparticles and free PS chains. Nanocomposite thin films on silicon substrates (pre-cleaned with piranha acid) were made by dip coating and then drying at 60 °C for 6 hours to remove solvent. After that pre-drying, the sample was annealed at 120 °C for 12 hours.

## **2.2 Characterization**

Molecular weight and PDI of polymers were determined by Tosoh EcoSEC GPC System. Polymer samples were made by dissolving P(MMA-*ran*-CHMA) in THF and the flow rate was 0.35 mL/min. Characterization was carried out at ambient temperature with a refractive index (RI) detector, two Tosoh TSKgel SuperMultiporeHZ-M columns (4.6 × 150 mm and 4 µm), and a TSKgel SuperMultiporeHZ-M guard column. The results were calibrated by PMMA standard method. <sup>1</sup>H NMR spectroscopy was done on a Liquid State Varian Mercury Vx 300 MHz NMR with polymer samples dissolved in deuterated chloroform (CDCl<sub>3</sub>). Glass transition temperatures of polymers and nanocomposites were measured on TA Instruments Q-2000 DSC by ramping the temperature from 30 to 130 °C at 10 °C/min using a heat/cool/heat cycle. The grafting density of chains on silica nanoparticles was determined from the weight loss measured using a TA Instruments Q-50 TGA. The test was performed in nitrogen with a heating rate of 10 °C/min from room

temperature to 500 °C. The morphologies of the polymer nanocomposites were imaged on Multimode Scanning Probe Microscope.

# **CHAPTER III**

## **RESULTS AND DISCUSSION**



In Chapter 2, methods for synthesizing P(MMA-*ran*-CHMA) random copolymers terminated with hydroxyl groups were described along with methods to prepare silica nanoparticles and graft P(MMA-*ran*-CHMA) polymer chains onto their surfaces. The strategy used to fabricate polymer nanocomposites by blending polymer-grafted nanoparticles with PS was also discussed. In this chapter, the characterization and results of the polymer brushes, nanoparticles, and the nanocomposites will be presented and discussed.

### 3.1 Characterization of P(MMA-*ran*-CHMA)

#### 3.1.1 Molecular weight and PDI

Various molecular weights of P(MMA-*ran*-CHMA) were synthesized by changing the amount of solvent, reaction temperature, and reaction time. Polymerization conditions are shown along with the resulting molecular weights and PDIs of the polymers in Table 3.1. Representative GPC traces of the different random copolymers are shown below in Figure 3.1.

**Table 3.1. Molecular weight of P(MMA-*ran*-CHMA) determined by GPC.**

Target $M_n$ kg/mol	Feed ratio $f_{\text{CHMA}} : f_{\text{MMA}}$	$M_n$ (g/mol)	$M_w$ (g/mol)	PDI
10	80:20	10020	11270	1.12
10	85:15	9870	11040	1.12
10	90:10	9950	11120	1.12
10	95:5	9970	11170	1.12
10	(Pure CHMA)	10110	11300	1.12
22	80:20	24560	26750	1.09
34	80:20	34760	36010	1.04

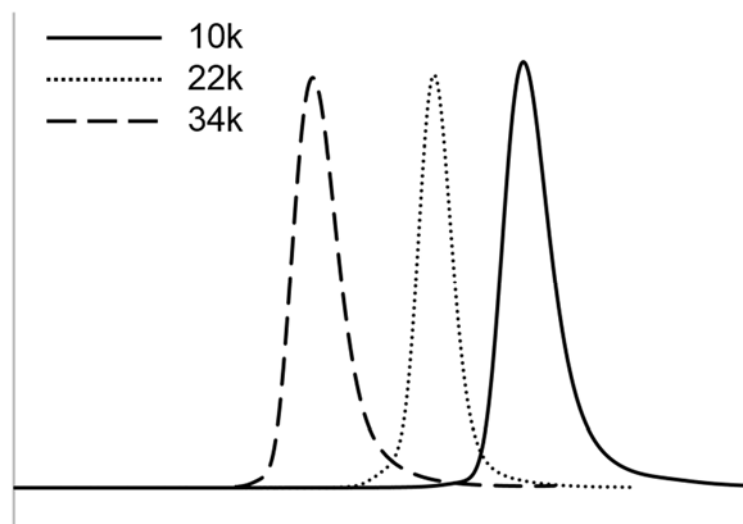


**Figure 3.1. GPC traces of P(MMA-*ran*-CHMA) with composition ratio 80:20 CHMA:MMA polymerized under different conditions.**

### ***3.1.2 Comonomer ratio of the random copolymers***

Because the random copolymers were made by ATRP in the presence of the two comonomers, it is important to know the ratio of MMA and CHMA in each random copolymer. Composition is important because PCHMA is miscible with PS while PMMA is not. Therefore, increasing the ratio of MMA relative to CHMA means that the random copolymer will be increasingly immiscible in the nanocomposites. Thus, controlling the incorporation of the two comonomers enables my investigations of the role of polymer composition on the  $T_g$  of the nanocomposites and the dispersion state of the copolymer grafted nanoparticles.

The monomer ratio was determined by  $^1\text{H}$  NMR spectroscopy. Figure 3.2 shows, as an example, the polymerization conducted with a feed ratio 80:20 CHMA:MMA. Spectra

were acquired from aliquots taken at 0 and 60 minutes of the reaction. Peak A, B, C, and D correspond to protons on the solvent, the cyclohexyl ring of CHMA, the methyl substituent of MMA, and the vinyls, respectively. Peak A was set as a reference since the amount of solvent remains constant during the polymerization – only the ratio of comonomers is changed.

The conversion of both monomers can be determined from the difference in the integrated signal from the relevant proton before and after the reaction. For example:

$$\text{conversion of CHMA} = (5.42 - 4.71) / 5.42 = 13.10 \%,$$

$$\text{conversion of MMA} = (3.41 - 2.98) / 3.41 = 12.61 \%,$$

While the peak used for MMA contains 3 protons dividing the integrated area by 3 makes no difference on the numerical results. From the calculated conversion, the degree of polymerization (DP) can be determined by the product of the calculated conversion and the ratio of monomer and initiator:

$$\text{DP of CHMA} = 13.10 \% \times 400 = 52.4,$$

$$\text{DP of MMA} = 12.61 \% \times 100 = 12.6.$$

With these results, the ratio of the comonomer in the polymer chains can be calculated in a straight-forward fashion:

$$52.4 / 12.6 = 4.16 = 80.62:19.38$$

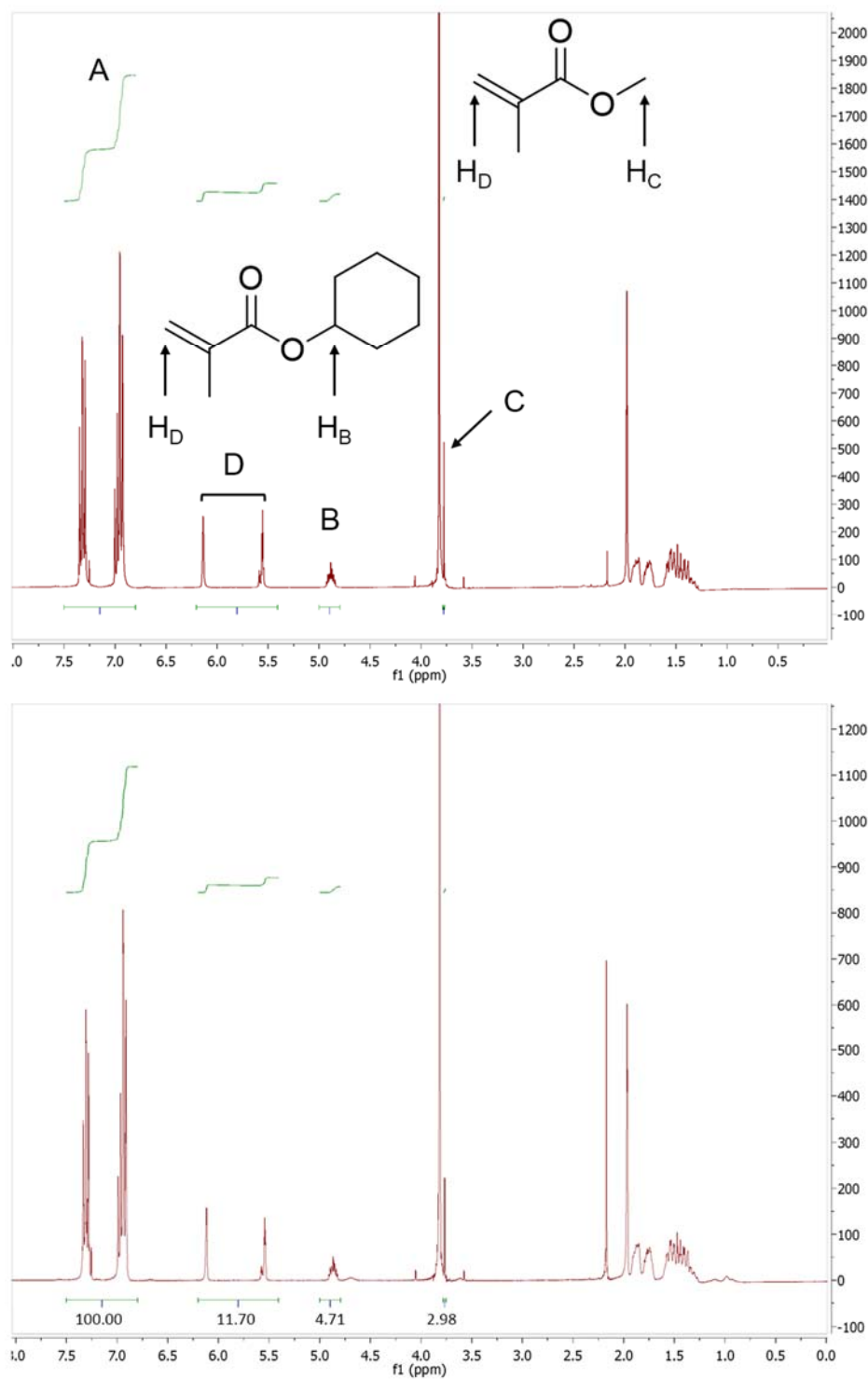


**Figure 3.2.**  $^1\text{H}$  NMR spectra of P(MMA-*ran*-CHMA) with feed ratio of 80:20 at the start (top) and the end (bottom) of the polymerization.

Using this analysis, I calculated the composition of the other random copolymers, and the results are listed in Table 3.2. The results show clearly that the incorporation of the monomers follows the feed ratio very closely for both lower molecular weight polymers and the few higher molecular samples made. This result provides further indication that the polymerization is well-controlled.

**Table 3.2. Composition of comonomers determined by  $^1\text{H}$  NMR.**

Feed ratio $f_{\text{CHMA}} : f_{\text{MMA}}$	Composition by NMR	$M_n$ (g/mol)	$M_w$ (g/mol)	PDI
80:20	80.62:19.38	10020	11270	1.12
85:15	85.25:14.75	9870	11040	1.12
90:10	90.20:9.80	9950	11120	1.12
95:5	95.23:4.77	9970	11170	1.12
(Pure CHMA)	/	10110	11300	1.12
80:20	79.33:20.67	24560	26750	1.09
80:20	81.16:18.84	34760	36010	1.04

## 3.2 Characterization of copolymer-grafted nanoparticles

### 3.2.1 Size of bare silica nanoparticles

The diameter of the nanoparticles is a key parameter affecting the miscibility of the copolymer-grafted nanoparticles. Dynamic light scattering was used to determine the size of the silica nanoparticles synthesized, and these measurements and data analysis were done by my colleague, Jesse Davis. The data, in the form of the apparent diffusion coefficient,  $D_{\text{app}}$ , are shown in Figure 3.3. These data, acquired at various scattering angles (which is expressed by  $q$ , where  $q = 4\pi\eta/\lambda \cdot \sin(\theta/2)$ ) can be used to determine the z-average diffusion coefficient by extrapolating to  $q = 0$ , the value of which can be used

with the Stokes-Einstein relation to determine the hydrodynamic radius,  $R_h$ . From this analysis, and as shown in Table 3.3, the radius of the silica nanoparticles were found to be 10 nm.

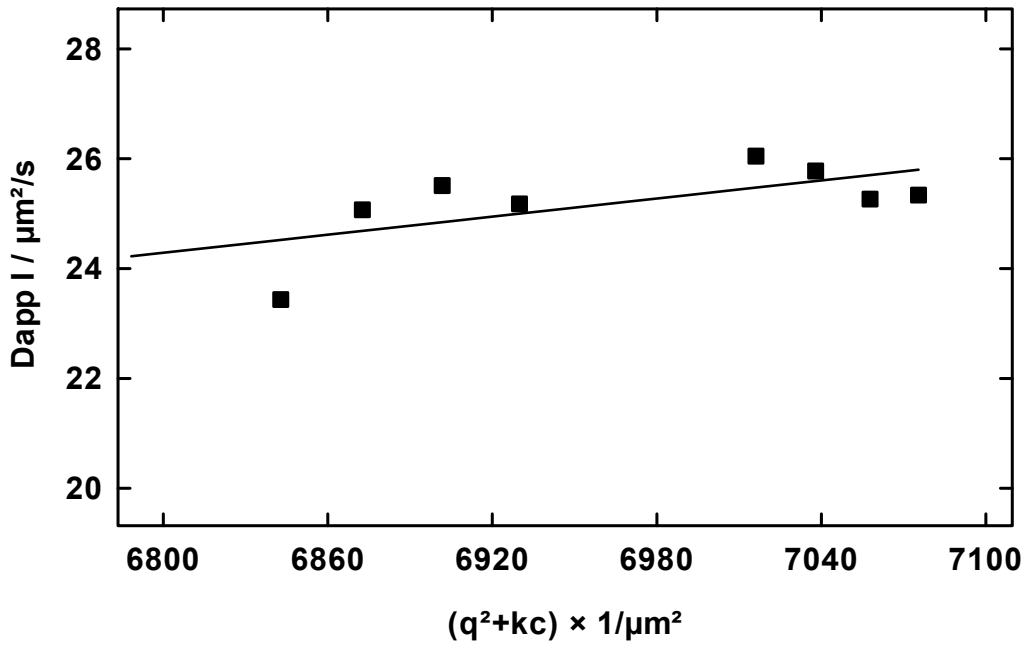


**Figure 3.3. Results of dynamic light scattering measurements of the silica nanoparticles in DI water.**

**Table 3.3. Calculated radius of the silica nanoparticles.**

Concentration (g/dm <sup>3</sup> )	Dz (μm <sup>2</sup> /s)	$R_h$ (nm)
64.9	2.23E+01	9.9

### ***3.2.2 Grafting density of copolymer-grafted nanoparticles***

Grafting density is another parameter that affects the miscibility of copolymer-grafted nanoparticles, so it is important to know how many polymer chains were grafted on each

kind of copolymer-grafted nanoparticles. One advantage of grafting to method is that the grafting density can be tuned by varying the reaction time. As the reaction time was held constant at 10 hours for each type of copolymer-grafted nanoparticles, I assume that measuring one sample was sufficiently representative of the grafting density of other copolymer-grafted nanoparticle made using polymers of the same molecular weight. Nanoparticles grafted with 10k P(MMA-*ran*-CHMA) (CHMA:MMA = 80:20) was characterized by TGA, and the curve is shown in Figure 3.4.

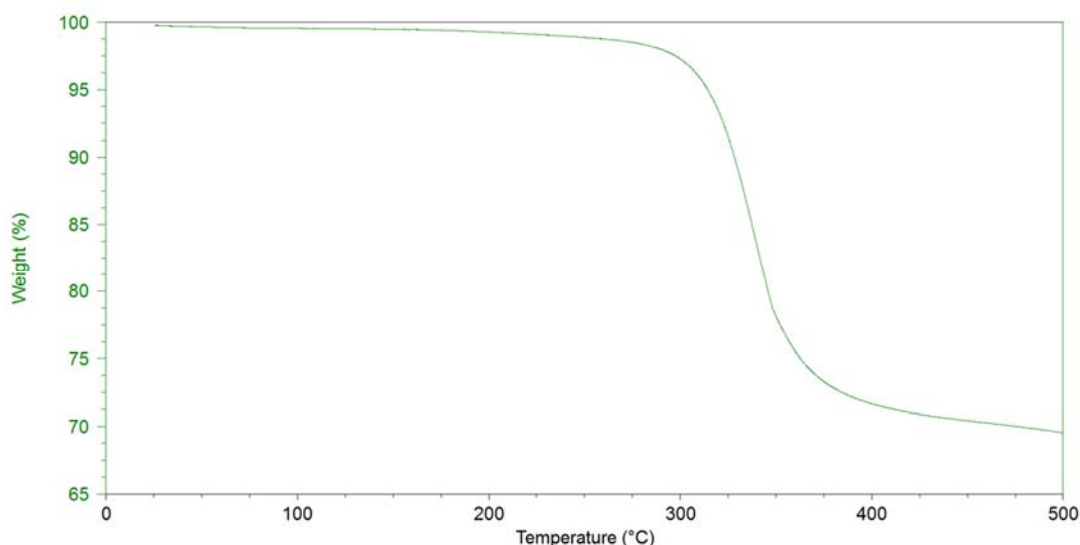


**Figure 3.4. TGA curve showing the mass loss of copolymer-grafted nanoparticles modified with 10k polymer brushes (CHMA:MMA 80:20).**

The mass of the sample was 5.812 mg before the measurement and 4.028 mg afterwards. 1.784 mg, which is attributed to the mass of polymer chains, was lost by thermal decomposition during the heating process, with the residue being the silica nanoparticles. To calculate the grafting density, the density of silica nanoparticles is also needed and it was determined by putting certain weight of dried silica nanoparticles in hexane (silica

nanoparticles are not soluble in hexane) and then measuring the change of volume. I did this with several different amounts of added silica nanoparticles in order to make a plot of volume versus mass. Because density is assumed to be constant, the slope of the line is the density of the nanoparticles. The data are shown in Table 3.4 and Figure 3.5, and the calculated density resulting from a linear regression is 2.49 g/mL.

**Table 3.4. Mass and volume data to determine the density of silica nanoparticles.**

Mass (g)	Volume (mL)
0.5	1.27
1.0	2.42
1.5	4.02
2.0	4.83
2.5	6.30

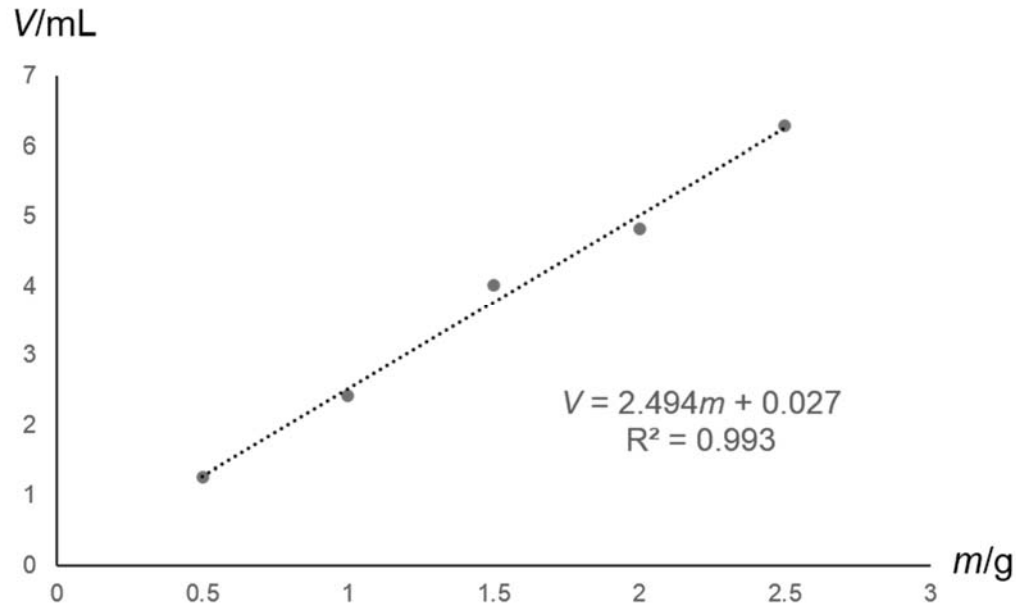


**Figure 3.5. A linear regression graph of volume versus mass. Density can be determined by the slope of the trend line.**



To calculate the grafting density, I need to know the number of polymer chains and the total surface area of the silica nanoparticles in the sample. The number of polymer chains can be calculated by the mass loss determined by TGA:

$$1.784 \text{ mg} / 1000 / 10020 \text{ g} \cdot \text{mol}^{-1} \times 6.02 \times 10^{23} \text{ mol}^{-1} = 1.07 \times 10^{17} \text{ chains.}$$

The surface area and volume of a silica nanoparticle with the radius of 10 nm are:

$$\text{Area} = 4\pi r^2 = 1256 \text{ nm}^2,$$

$$\text{Volume} = 4 \pi r^3 / 3 = 4188 \text{ nm}^3.$$

The total volume of the silica nanoparticles in the sample can be calculated by the mass of the residue and the density:

$$4.028 \text{ mg} / 1000 / 2.49 \text{ g} \cdot \text{mL}^{-1} = 1.62 \times 10^{-3} \text{ mL} = 1.62 \times 10^{18} \text{ nm}^3.$$

Then the number of silica particles in the sample is determined by the total volume divided by the individual volume:

$$1.62 \times 10^{18} \text{ nm}^3 / 4188 \text{ nm}^3 = 3.87 \times 10^{14},$$

so the total surface area is the product of the number and the surface area of individual silica nanoparticle:

$$3.87 \times 10^{14} \times 1256 \text{ nm}^2 = 4.86 \times 10^{17} \text{ nm}^2.$$

With these results, the grafting density of the copolymer-grafted nanoparticles can be calculated:

$$1.07 \times 10^{17} \text{ chains} / 4.86 \times 10^{17} \text{ nm}^2 = 0.22 \text{ polymer chains per nm}^2.$$

A TGA test of epoxy-coated nanoparticles was also conducted to determine the ratio of impurities in nanoparticles (Figure 3.6).

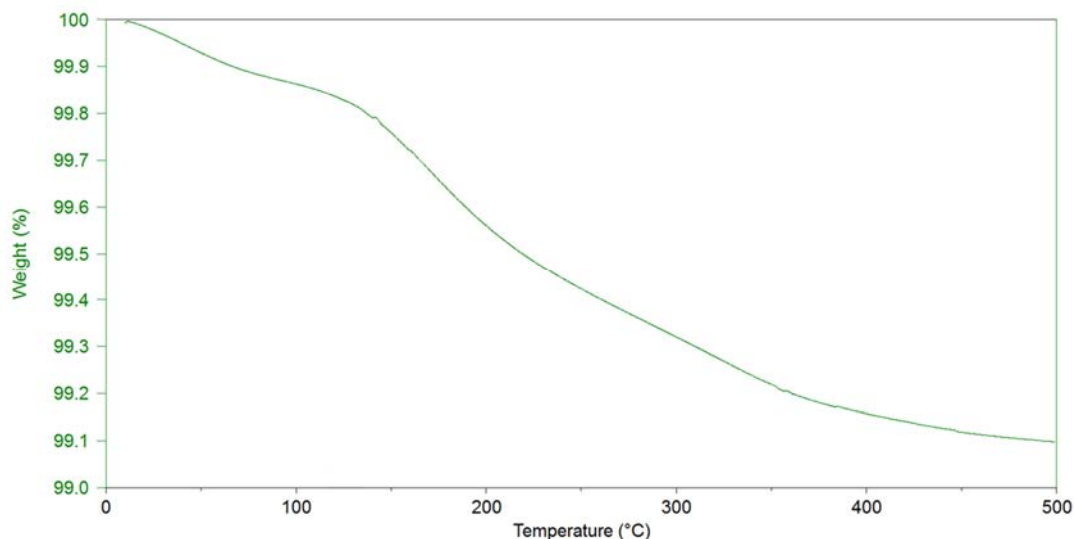


**Figure 3.6. TGA curve showing the mass loss of epoxy-coated nanoparticles.**

From the graph, the mass loss was 0.9 %, which is the ratio of impurities of epoxy-coated nanoparticles. The calibrated grafting density remains the same, 0.22 polymer chains per  $\text{nm}^2$ .

With the grafting density of one type of copolymer-grafted nanoparticles determined, the grafting densities of the other types were assumed to be the same or close to this result.

### **3.3 Characterization of polymer nanocomposites**

#### ***3.3.1 Glass transition temperature***

One goal of my work is to investigate the role of copolymer-grafted nanoparticles with various brush compositions on the glass transition temperature of the polymer matrix.

Glass transition temperature can be measured by DSC. Through the data and graphs

shown below (Figure 3.7 and Table 3.5), the influence of copolymer-grafted nanoparticles on the  $T_g$  of PS nanocomposites is revealed.

**Table 3.5. Glass transition temperature of nanocomposites samples.**

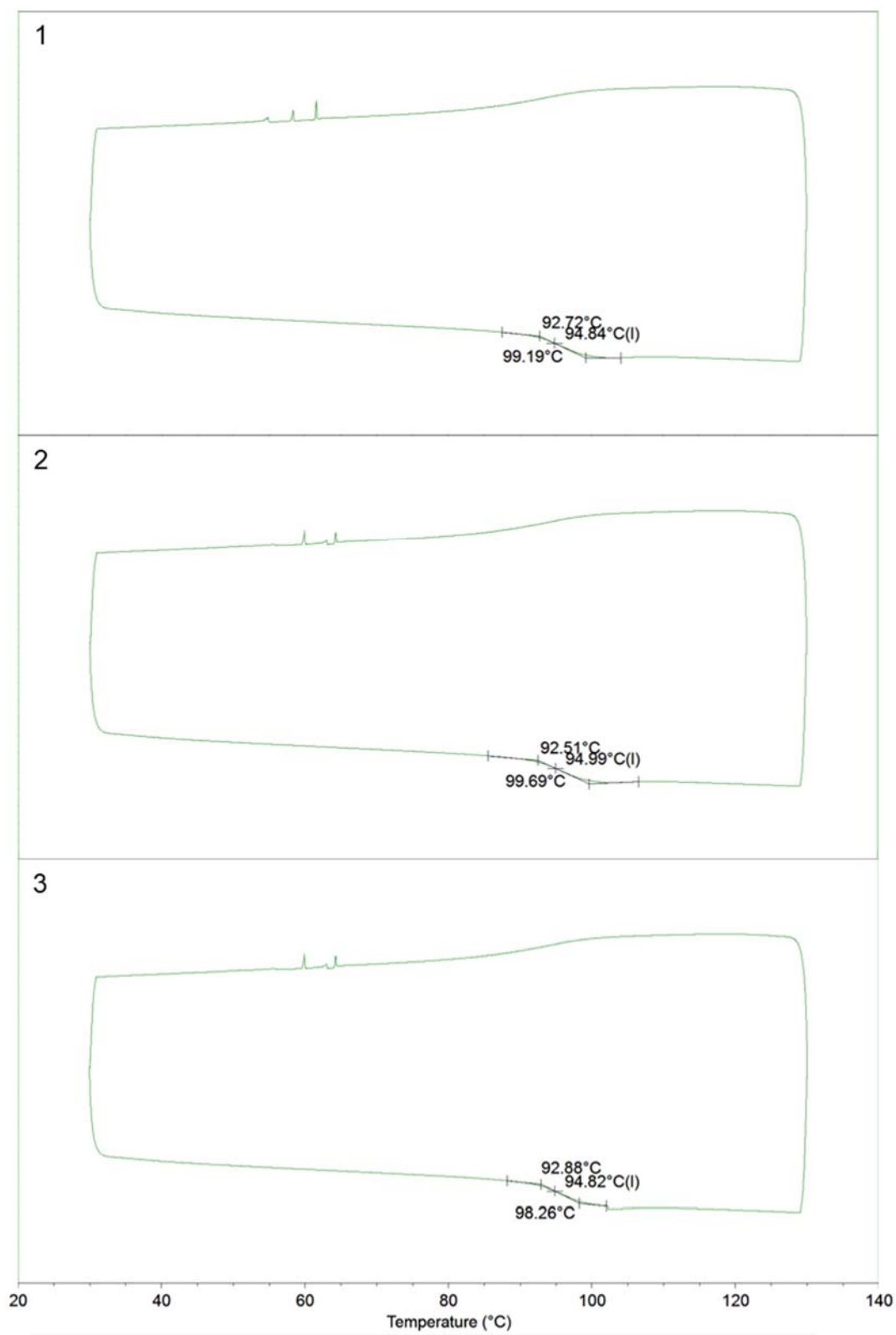
No.	$M_n$ of PS	Copolymer-grafted nanoparticles	$T_g$ (°C)
1	18k	None	95
2	18k	10k brushes with the ratio 80:20	95
3	18k	10k brushes with the ratio 85:15	95
4	18k	10k brushes with the ratio 90:10	95
5	18k	10k brushes with the ratio 95:5	95
6	18k	10k brushes of PCHMA	95
7	26k	None	104
8	26k	22k brushes with the ratio 80:20	104
9	48k	None	106
10	48k	34k brushes with the ratio 80:20	106

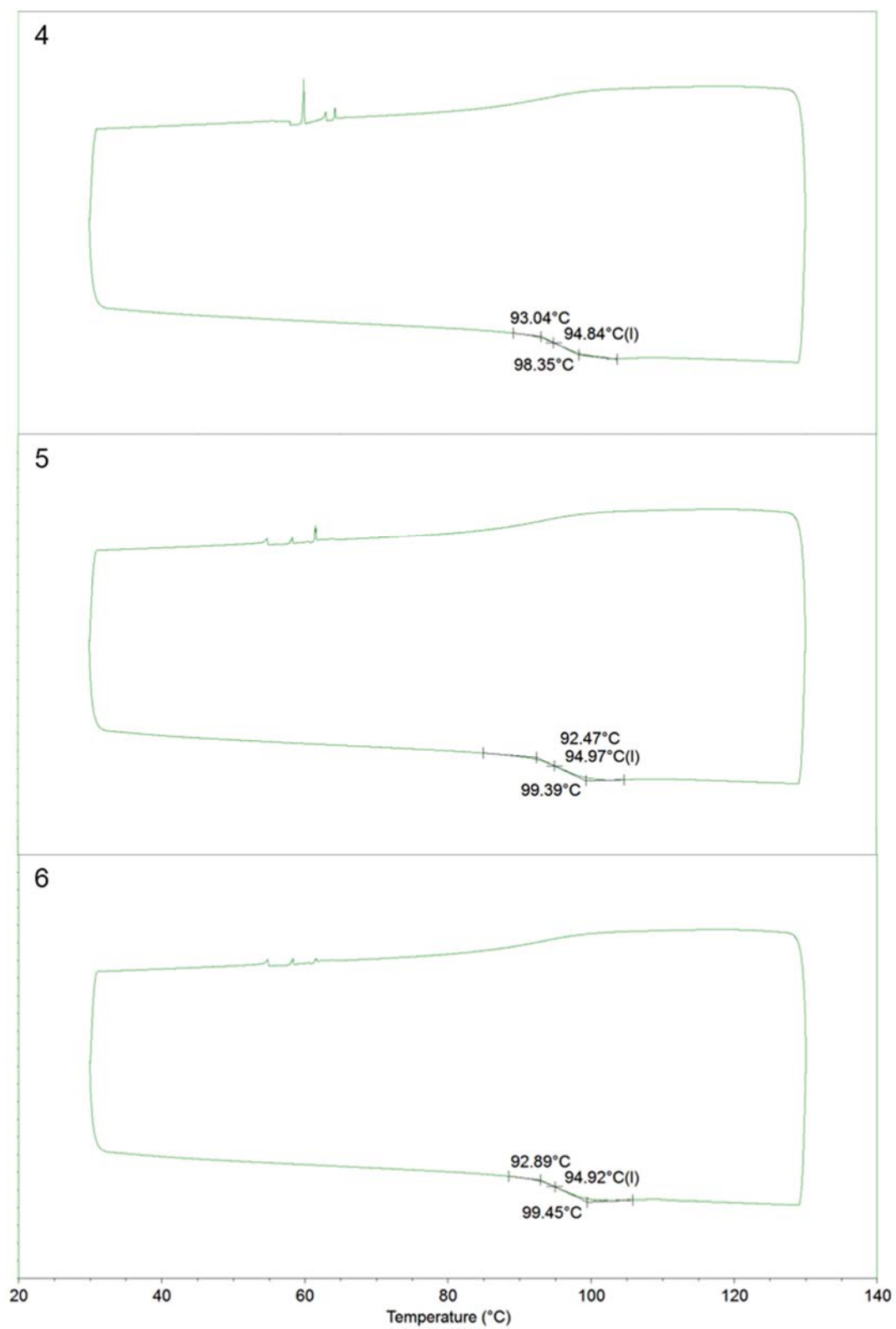
From the results, no significant influence on the  $T_g$  of PS was observed after blended with copolymer-grafted nanoparticles. This can be explained that the  $T_g$  of PS, PMMA and PCHMA are fairly close (all around 105°C),<sup>21, 22</sup> so the resulting  $T_g$  of mixture of these three polymers actually remains unchanged.

### ***3.3.2 Dispersion state of nanoparticles in polymer matrices***

As suggested above, PS is miscible with PCHMA while immiscible with PMMA. Increasing the ratio of MMA to CHMA means that the random copolymer becomes increasingly immiscible in the PS nanocomposites. To reflect the influence of brush composition on the spatial distribution of the copolymer-grafted nanoparticles in polymer matrices, PS nanocomposites blended with 10k copolymer-grafted nanoparticles were

**Figure 3.7. DSC curves of 18k PS and 18k PS blended with nanoparticles grafted with 10k brushes of various composition. Sample numbers correspond to those in Table 3.5. Data was analyzed using *TA Universal Analysis* software.**





imaged before and after annealing by atomic force microscopy (Figure 3.8).

As discussed in Chapter 1, the miscibility of polymer-grafted nanoparticles are high when wet brush conditions ( $N > P$ ) are met and low when dry brush conditions dominate ( $N < P$ ). For all the PS nanocomposites imaged, the molecular weight of PS matrix was 18k and the copolymer brushes were 10k. In this situation, dry brush conditions are met and the copolymer-grafted nanoparticles are expected to be immiscible with PS matrices.

However, only Sample 5, with brush composition of 80:20 CHMA:MMA, appears to show any evidence of immiscibility, as aggregates consisting of a few nanoparticles were observed in the image after annealing. The cause of this observation may be that at higher ratio of CHMA in the polymer brush, enthalpy dominates. Even though  $N < P$ , the enthalpic interaction is favored by the system which drives the polymer brush to mix with PS. But when the ratio of CHMA:MMA reaches 80:20, the enthalpic contribution is not strong enough to overcome entropy (the classic demixing expected with homopolymer-grafted nanoparticle/homopolymer matrix system), and the system shows signs of phase separation.

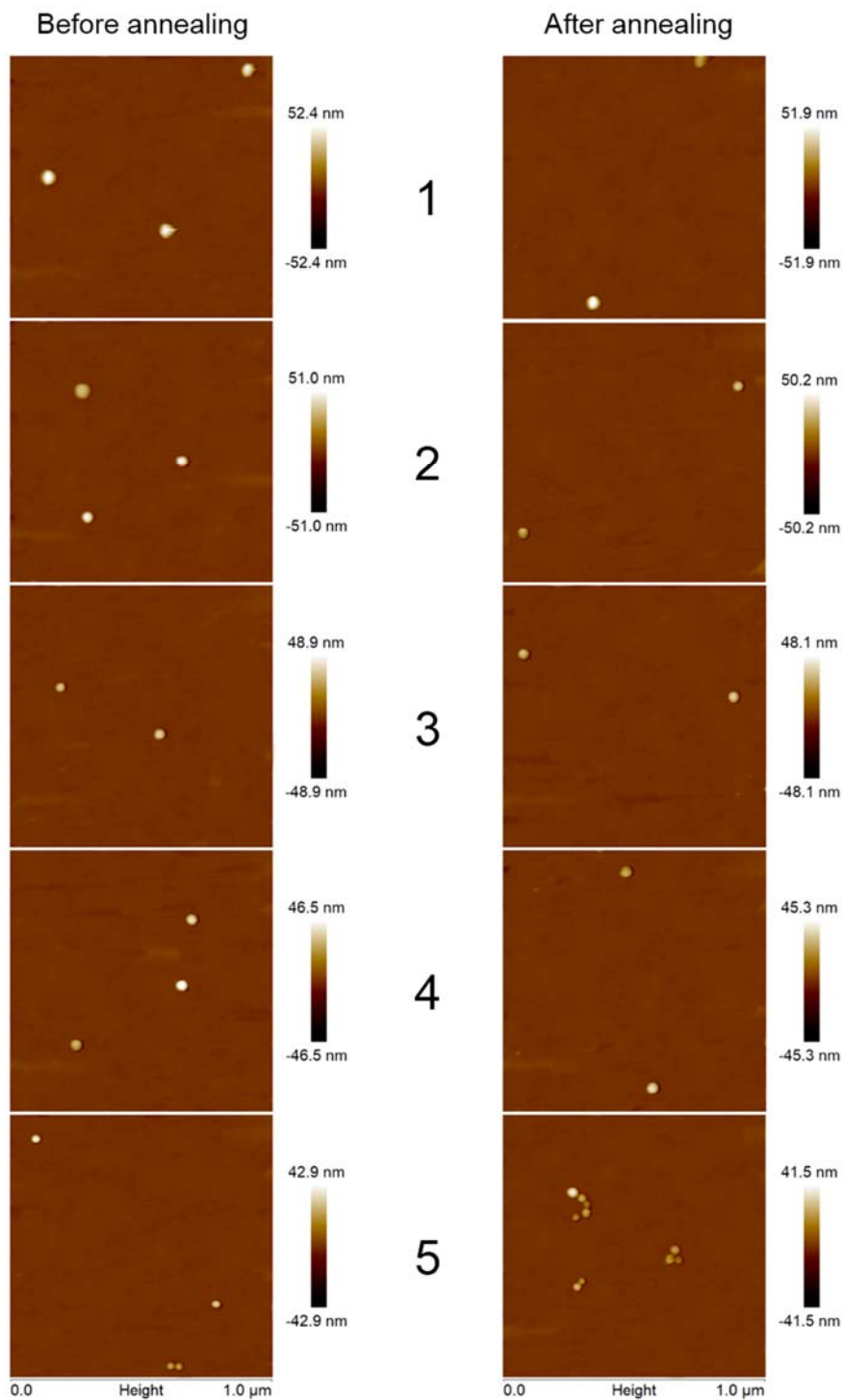


**Figure 3.8. AFM images of PS nanocomposites made with 10k copolymer-grafted nanoparticles in a matrix of 18k. The loading ratio is 2 wt. %. From 1 to 5, the ratios of MMA units in the brush are: 0%, 5%, 10%, 15%, and 20%.**



**CHAPTER IV**

**CONCLUSIONS AND FUTURE WORK**

## 4.1 Conclusion

A series of experiments and characterizations were conducted to study the PS based nanocomposites with copolymer-grafted nanoparticles because of their advantages over the homopolymer-grafted nanoparticles in tunability in polymer brush composition. Silica nanoparticles grafted with random copolymers, P(MMA-*ran*-CHMA), of various molecular weight and composition were synthesized and dispersed in PS matrices. The role of the copolymer-grafted nanoparticles on the glass transition temperature of the PS/nanoparticle composite and the spatial distribution of the nanoparticles were studied in this work. The addition of copolymer-grafted nanoparticles showed no influence on the  $T_g$  of PS nanocomposites since the  $T_g$  of PS, PMMA, and PCHMA are fairly close to one another. As a result, mixing the copolymer grafted nanoparticles does not change the  $T_g$  of the PS, which is the dominant component of the nanocomposite system. On the other aspect, the PS nanocomposites with copolymer-grafted nanoparticles of brush composition ratio MMA:CHMA lower than 20:80 can form a homogeneous thin film, while the higher ratio shows signs of separation as aggregation was observed in AFM images. This is mainly due to that as the ratio of MMA becomes higher, the enthalpic interaction overcomes the entropic forces that drive the random copolymer brushes to mix with the polymer matrix, and as a result, the system shows heterogeneity.

## 4.2 Future work

In my research, PS based nanocomposites with random copolymer-grafted nanoparticles were studied via AFM and DSC. It would be beneficial to make other tests of the nanocomposites to examine their mechanical properties. One possible method is to use dynamic mechanical analysis (DMA), which can provide insight into the influence of brush composition on mechanical properties such as modulus of the nanocomposites.

Grafting density can be a parameter that affects the miscibility of polymer-grafted nanoparticles. In my work, the copolymer-grafted nanoparticles were all prepared at a single grafting density. To fabricate nanocomposites with copolymer-grafted nanoparticles of varying grafting density would be an interesting effort, as the role of grafting density on the mechanical and physical properties of polymer matrix and the dispersion state of the polymer-grafted nanoparticles can be studied. It stands to reason that grafting density affects the extent to which free (matrix) chains can penetrate into the brush, so I would expect thermomechanical properties to change as grafting density is changed.

There are many other studies to examine the morphology that should be performed. AFM is a relatively easy characterization method, but it looks at the surface only. Thus it provides an incomplete picture of nanocomposite morphology. Other morphologies studies can be conducted: For example, the systems I prepared and studies can be compared with the behaviors of nanoparticles grafted with P(MMA-*b*-CHMA) diblock

copolymers dispersed in a homopolymer PS matrix or a homopolymer blend matrix.

Random copolymers, P(MMA-*ran*-CHMA), with two or more different chain lengths grafted on the same nanoparticles would be interesting to investigate, then there would be three conditions based on the relative chain lengths to look into:  $N_1 < N_2 < P$ ,  $N_1 < P < N_2$ , and  $P < N_1 < N_2$ . There remains a lot of interesting and mysterious areas to be explored in this field.

## REFERENCE

1. Dukes, D.; Kalb, J.; Kumar, S. K.; Hoy, R. S.; Grest, G. S. *Soft Matter* **2011**, *7*, 1418.
2. Hall, L. M.; Jayaraman, A.; Schweizer, K. S. *Curr. Opin. Solid State Mater. Sci.* **2010**, *14*, 38.
3. Ellison, C. J.; Pryamitsyn, V.; Ganesan, V. *Soft Matter* **2010**, *6*, 4010.
4. Payne, A. R. *J. Appl. Polym. Sci.* **1965**, *9*(6), 2273-2284.
5. Ginzburg, V. V. *Macromolecules* **2005**, *38*, 2362.
6. Israelachvili, J. *Intermolecular and Surface Forces, Chapter 13* Academic Press, New York, 2<sup>nd</sup> edition, 1985.
7. Kim, J.; Green, P. F. *Macromolecules* **2010**, *43*, 1524.
8. Mackay, M. E.; Tuteja, A.; Duxbury, P. M.; Hawker, C. J.; Horn, B. V.; Guan, Z.; Chen, G.; Krishnan, R. S. *Science* **2006**, *311*, 1740.
9. Borukhov, I.; Leibler, L. *Macromolecules* **2002**, *35*, 5171.
10. Nodoro, T. V. M.; Voyiatzis, E.; Ghanbari, A.; Theodorou, D. N.; Bohm, M. C.; Muller-Plathe, F. *Macromolecules* **2011**, *44*, 2316.
11. Pyramtisyn, V.; Ganesan, V.; Panagiotopoulos, A. Z.; Liu, H.; Kumar, S. K. *J. Chem. Phys.* **2009**, *131*, 221102.
12. Barbey, R.; Lavanant, L.; Paripovic, D.; Schüwer, N.; Sugnaux, C.; Tugulu, S.; Klok, H.A. *Chem. Rev.* **2009**, *109*, 5437.
13. Goel, V.; Chatterjee, T.; Bombalski, L.; Yurekli, K.; Matyjaszewski, K.; Krishnamoorti, R. *J. Polym. Sci. Part B: Polym. Phys.* **2006**, *44*, 2014.
14. Zhao, Y. L.; Perrier, S. *Macromolecules* **2006**, *39*, 8603.

15. Jayaraman, A. *J. Polym. Sci. Part B: Polym. Phys.* **2013**, *51*, 524.
16. Martin, T. B.; McKinney, C.; Jayaraman, A. *Soft Matter* **2013**, *9*, 155.
17. Kim, J. H.; Park, D. S.; Kim, C. K. *J. Polym. Sci. Part B: Polym. Phys.* **2000**, *38*, 2666.
18. Matyjaszewski, K.; Jianhui, X. *Chem. Rev.* **2011**, *101*, 2921.
19. Hartlen, K. D.; Athanasopoulos, A. P. T.; Kitaev, V. *Langmuir* **2008**, *24*, 1714.
20. Lin, J.; Siddiqui, J. A.; Ottenbrite, R. M. *Polym. Adv. Technol.* **2001**, *12*, 285.
21. Rieger, J. *Journal of Thermal Analysis* **1996**, *46*, 965.
22. Min, K. E.; Lee, D. H.; Jung, H. M. *Polymer Bulletin* **1990**, *24*, 221.

## **VITA**

Jiadi Hou was born in Changchun, China in the year of horse, 1990. He graduated from Jilin University with a bachelor degree in chemical engineering in June of 2013. He came to the United States and pursued his Master of Science degree in Chemistry at the University of Tennessee, Knoxville in August, 2013. He joined Dr. Mike Kilbey's group in January 2014 and focused his research on advanced polymer nanocomposites made with copolymer-decorated nanoparticles. After graduation he plans to pursue an advanced degree in computer science at University of North Carolina-Charlotte.